



## Analyzing Bornova Plain's Basin Structure Using Density Parameter

\*Makale Bilgisi / Article Info

Alındı/Received: 09.06.2023

Kabul/Accepted: 21.01.2024

Yayımlandı/Published: 27.02.2024

### Bornova Ovası'nın Havza Yapısının Yoğunluk Parametresi Kullanılarak Analizi

Yaprak ÖZDAĞ<sup>1\*</sup>, Oya ANKAYA PAMUKÇU<sup>1,2</sup>

<sup>1</sup>Department of Geophysics Engineering, The Graduate School of Natural and Applied Sciences, Dokuz Eylül University, İzmir, 35390, Türkiye

<sup>2</sup>Department of Geophysics Engineering, Engineering Faculty, Dokuz Eylül University, İzmir, Türkiye

© Afyon Kocatepe Üniversitesi

#### Abstract

Due to the tectonic regime it has been subjected to under the influence of Western Anatolia, the area contains numerous sedimentary basin structures. The study area, located within the province of İzmir, is a region where a significant number of historical and instrumental earthquakes have occurred due to its tectonic structure. The Bornova Plain, located east of the inner Gulf of İzmir, is highly susceptible to earthquakes due to dense urbanization. This was clearly observed during the Samos earthquake on October 30, 2020. In this study, a microgravity field survey was conducted in a larger area than previous studies to better characterize the basin effect of the plain and obtain a high-resolution dataset representing a wide area. The necessary measurement point distribution was performed with a variable sampling interval of approximately 200-1000 meters, resulting in a microgravity dataset of 458 points. By taking 1 profile section from the residual Bouguer gravity map created for the Bornova Plain, inverse solution modeling was performed. The density values obtained from the inverse solution modeling were compared with the densities calculated from seismic velocities obtained through the spatial autocorrelation (SPAC) method conducted in the study area. A high consistency was observed between the density values obtained from the two different methods compared.

**Anahtar Kelimeler:** Bornova Basin; Gravity; SPAC; Density; Velocity.

#### Öz

Batı Anadolu etkisinde kaldığı açılma rejimi nedeniyle birçok sedimanter havza yapısı içerir. Çalışma alanını içeren İzmir ili tektonik yapısından dolayı tarihsel ve aletsel dönemde çok sayıda depremin gerçekleştiği bir bölgedir. İzmir iç körfezinin doğusunda yer alan Bornova Ovası üzerinde bulunan yoğun yapılaşma nedeniyle yüksek bir deprem riskine sahiptir. Bu durum 30 Ekim 2020'de gerçekleşen Samos depremi ile açık bir şekilde gözlenmiştir. Bu çalışma kapsamında geçmiş çalışmalarından daha büyük bir alanda mikrogravite saha çalışması gerçekleştirilerek ovanın havza etkisini daha iyi niteleyebilecek, çözünürlüğü yüksek ve geniş bir alanı temsil edecek şekilde bir veri seti elde edilmiştir. Bu kapsamda gerekli ölçüm nokta dağılımı yaklaşık 200-1000 m'lik değişken bir örnekleme aralığı ile yapılmış olup toplam 458 noktalık bir mikrogravite veri seti oluşturulmuştur. Bu çalışma kapsamında Bornova Ovası için oluşturulan rezidüel Bouguer gravite haritası üzerinden 1 profil kesiti alınarak, ters çözüm modellemesi gerçekleştirilmiştir. Gerçekleştirilen ters çözüm modelleme sonucu yoğunluk değerleri ile çalışma alanında gerçekleştirilen derin uzaysal özilişki yönteminden (SPAC) elde edilen sismik hızlardan hesaplanan yoğunluklar karşılaştırılmıştır. Karşılaştırılan 2 farklı yöntem ile elde edilen yoğunluk değerleri arasında yüksek bir uyum gözlenmiştir.

**Keywords:** Bornova Havzası; Gravite; SPAC; Yoğunluk; Hız.

#### 1. Introduction

The Bornova Plain has been studied by various researchers in terms of natural disasters due to its basin structure and rapid urbanization over the past 50 years. Akgün et al. (2013a) evaluated the data obtained from previous studies (microgravity, borehole seismic surveys, SPAC, etc.) for the Bornova Plain and observed that the engineering bedrock ( $V_s > 760$  m/s) depth is approximately 400 meters in the coastal areas. Another study conducted specifically for the Bornova Plain is by Özdağ et al. (2015), where calculations of dynamic amplification factor distribution were performed using

the microtremor method. The results of this study indicate that the dominant vibration period of the ground in the coastal areas of the Bornova Plain ranges up to 5 seconds, and the dynamic ground amplification factor can reach up to 3.5 times. It was concluded that the seismic bedrock ( $V_s > 3000$  m/s) interface is located at an average depth of 1500 meters. Following these studies, Pamuk et al. (2017 and 2018) conducted studies in the plain, where a selected area of 6x10 km was modeled in 2D using microgravity and SPAC methods on 7 profiles with a strike direction. By interpolating these profiles, a 3D model was created, revealing the overall basin structure of the Bornova Plain. The common point

of all these studies is that the deep alluvial deposits in the Bornova Plain, under the influence of dynamic forces (earthquakes), can negatively affect urbanization due to changes in the amplitude and frequency content of the resulting earthquake. The deep soil boreholes conducted in the Bornova Plain after the studies by Pamuk et al. (2017 and 2018) highlighted the need for updating the models obtained from these studies. In this study, a high-resolution microgravity dataset was obtained for the Bornova Plain, and a modeling study was conducted by applying inverse solution modeling on a profile section obtained from the Bouguer anomaly map resulting from corrections applied to this dataset. The density values obtained from the model were compared with the density values calculated from the spatial autocorrelation (SPAC) method based on S-wave velocity models given in Özdağ's study (2022).

## 2. Study Area

The Bornova Plain is a basin located within an area bounded by the Yamanlar Elevation to the north, the Nif Elevation to the south, Kemalpaşa to the east, and the Gulf of Izmir to the west.

The Bornova Complex Unit constitutes the bedrock of the Bornova Plain. Due to intense deformation resulting from tectonic activities, a high degree of structural change has been observed compared to earlier times (Erdoğan, 1990). The streams flowing from the northern and southern elevations of Bornova deposit their coarse load as alluvial fans in the foothills and spread the low-energy fine sediment load over the plain (Kayan, 2000). Additionally, Holocene coastal developments, similar to those observed along the entire Western Anatolian coast, have been observed in the coastal areas of Bornova. Therefore, a coastal strip has formed as an extension of the plain located behind the delta on the Bornova coast (Kayan, 2000). In particular, data from deep drilling conducted by the State Hydraulic Works (DSİ) in the Bornova Basin provide evidence of the presence of likely Plio-Pleistocene sediments beneath the Holocene fill, with a total thickness of these deposits reported to exceed 200 meters (Karadaş, 2014). Additionally, the basin is bounded by the Karşıyaka Fault Zone to the north and the Izmir Fault Zone to the south.

## 2. Materials and Methods

Gravity method is considered a useful geophysical method in terms of cost and practicality. This method is based on the principle that the density of rocks that make up the Earth's crust decreases or increases at any

point, known as the natural source potential field method. Microgravity refers to anomaly measurements in gravity surveys that are smaller than 0.1 mGal. The development of this method initially involved calculations for the average density and mass of the Earth. The foundation of the gravity method is based on density differences between rocks with generally low and uniform density variations, resulting in small and smooth gravity anomalies. The small scale of these variations necessitates highly sensitive gravity measurements. Due to the heterogeneous structure of the Earth, the gravity acceleration is not constant over the entire surface of the Earth. The magnitude of gravity acceleration is primarily influenced by five factors: latitude, elevation, topography, Earth's oscillations, and density variations in the subsurface. Therefore, various corrections need to be applied to gravity measurements to remove unwanted components. Common corrections applied to gravity data obtained on land include drift correction, topographic correction, and Bouguer correction.

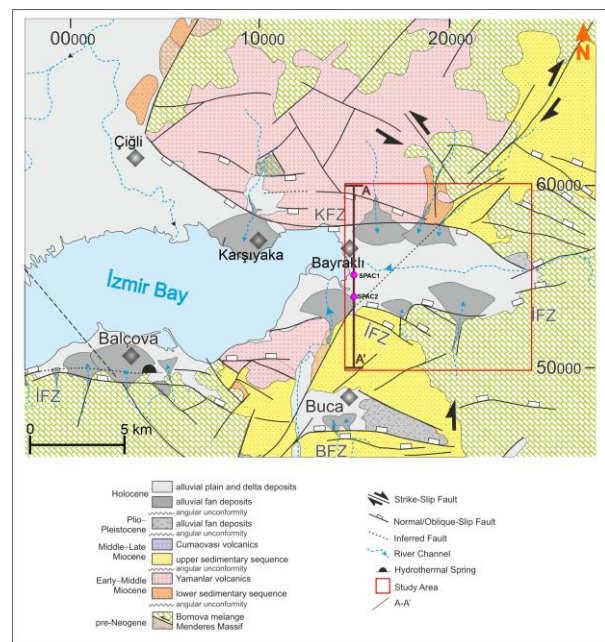


Figure 1. Geological map of study area (Modified from Uzel et al. (2012))

## 3. Results

In previous studies for the Bornova Basin, microgravity field surveys were conducted within an approximate area of 60 km<sup>2</sup> with a measurement interval of 1 km (Pamuk et al., 2017 and 2018). In this study, in addition to the existing measurements, an additional area of approximately 21 km<sup>2</sup> was surveyed, resulting in a total of 458 points with a sampling interval of 200-1000 m to better characterize the basin's influence on the plain.

The field surveys were conducted using a Scintrex CG-5 Autograv gravimeter with 3 repetitions and a measurement duration of 60 seconds. Corrections including drift correction, topographic correction, and Bouguer correction were applied to the obtained dataset using a 1st-degree polynomial equation. For topographic data, SRTM data with a sampling interval of 30 m was used (Figure 2).



**Figure 2.** Study Area SRTM Topographic Map with Microgravity Measurement Points.

$$gB = gobs \pm dgL + 0.3086 \Delta h - (0.04191\rho)\Delta h + dgT \quad (1)$$

dgL: Latitude correction

dgT: Topography correction

0.3086 Δh: Free-air correction

(0.04191ρ)Δh: Bouguer correction

After obtaining the complete Bouguer data (Figure 3), regional residual separation processes were performed using WingLink software.

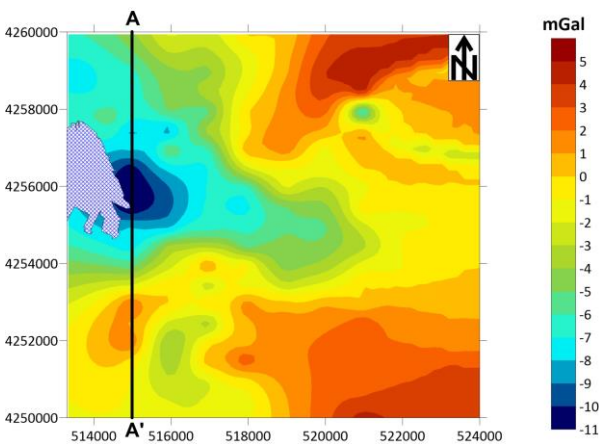


**Figure 3.** Study Area Complete Bouguer Map

After applying a 4th-degree polynomial trend to the complete Bouguer data, the residual Bouguer anomaly map was obtained (Figure 4).

Modeling stages were performed using the Grablox V1.6b software provided in the study by Pirttijavi (2008). The software is capable of calculating the synthetic gravity anomaly of a three-dimensional block model (direct solution) as well as calculating the 3D density model of a known area from gravity anomaly data (inverse solution). As shown in Figure 5, the software divides a 3D volume into blocks and performs calculations, allowing for increased resolution by determining the block sizes.

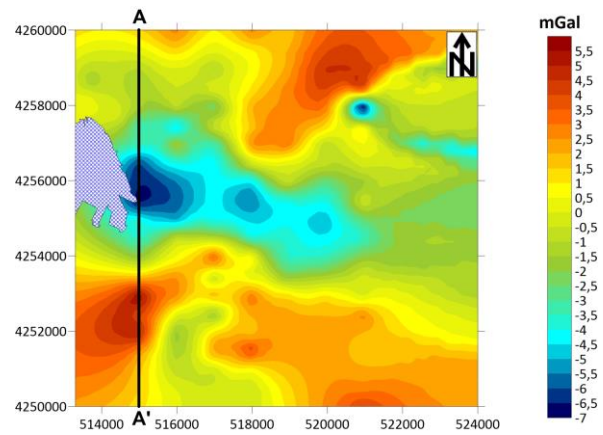


**Figure 4.** Study Area Residual Bouguer Anomaly Map

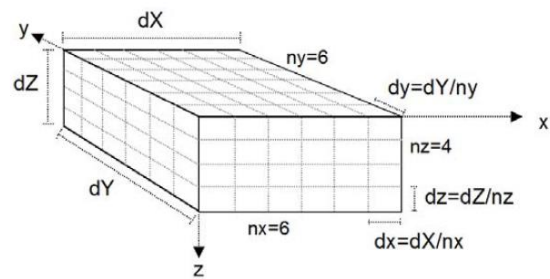


**Figure 5.** 3D Block Study

The working principle of the software can be summarized as follows: In the first stage of the inverse solution, gravity anomaly values for a known field are defined in the program. Then, the expected density values within a certain range are defined to create a limited initial model. Subsequently, the solution is obtained using Singular Value Decomposition (adaptive damping) (Van Loan 1976, Stewart 1993, Baker 2005) and Occam's Principles (minimizing model roughness

and inconsistency) (Constable et al. 1987, Chen et al. 2017).

After deciding to use the Grablox software for modeling, it was decided to evaluate the success of the inverse solution by calculating the gravity anomaly of a simple cube model with specific dimensions and density (direct solution) using the program. For this purpose, a rectangular prism with dimensions of approximately 10x10 km in the x-y plane and extending from 1 km depth to 5 km depth with a density of 3 g/cm<sup>3</sup> (Figure 6) was subjected to the direct solution process using the Potensoft software (Arisoy and Dikmen 2011), and the gravity anomaly map of the corresponding structure was calculated (Figure 7) within a 50x50 km area.

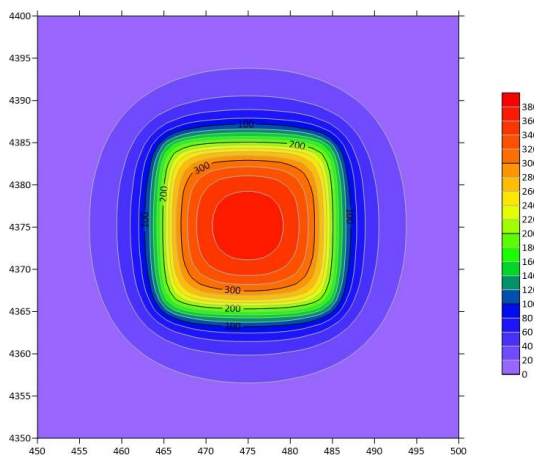


**Figure 7.** Gravity anomaly map generated using the Potensoft program for the structure in the form of a rectangular prism.

After performing the straight inversion modeling as shown in Figures 6 and 7, various inverse solution processes were applied using the GRABLOX 1.6b program to investigate its solution capacity (Figure 8). This allowed the reliability of the software to be assessed for modeling real field data. Despite some scatter due to the sharpness of the modeled structure on both sides of the structure, it was observed that the software successfully determined the density and geometric shape of the modeled prism with high accuracy.

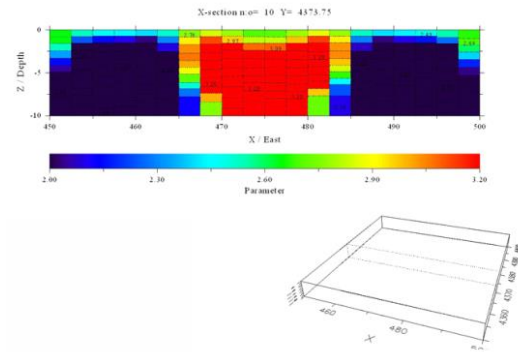


**Figure 8.** Cross-section of the 3D model created through inverse solution processes in GRABLOX 1.6b program.

During the data modeling stage, the residual Bouguer gravity map provided in Figure 4 was inputted into the software to obtain a high-resolution model. Calculations were performed with a cell size of 200x200 m. Previous studies (Pamuk et al., 2018; Özdağ, 2022) in the study area were taken into account, and density values ranging from 1.6 to 3 g/cm<sup>3</sup> were defined as input parameters. The resulting data were visualized by gridding the calculated values using Surfer software, and a 2D subsurface density model for the A-A' profile was obtained, as shown in Figure 9.

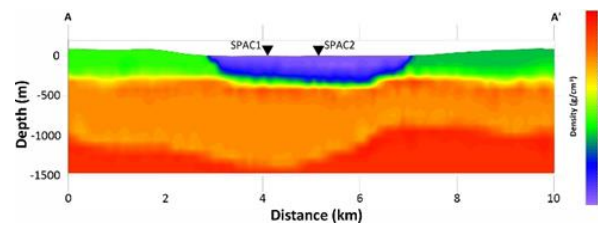


**Figure 9.** 2D subsurface density model for the A-A' profile.

The density values obtained from the empirical relationship (Equation 2) (Keçeli 2009) using the S-wave velocities derived from the spatial correlation method data (Figure 1 and 2) in Özdağ's study (2022) were utilized for density comparison. The density values obtained through this approach are presented in Figure 11, 12, 13, and 14.

$$\rho = 0,44 \times Vs(0,25) \quad (2)$$

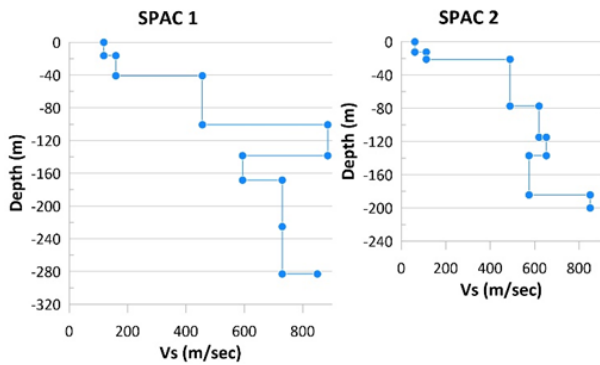


**Figure 10.** Depth Variation of S-Wave Velocity for SPAC 1 and SPAC 2 Points from Özdağ's study (2022)

The correlation coefficient is a statistical measure that quantifies the degree of relationship between two variables. This measure indicates a linear relationship between the variables and determines how much they vary together. The correlation coefficient takes a value between -1 and 1. A value of -1 indicates a perfect negative correlation, while 1 indicates a perfect positive correlation. A value of 0 indicates no relationship between the two variables. The correlation coefficient is an important tool for data analysis and understanding, and as a result, it is widely used by researchers and decision-makers (Asuero et al., 2006; Taylor, 1990; Ratner, 2009; Mukaka, 2012).

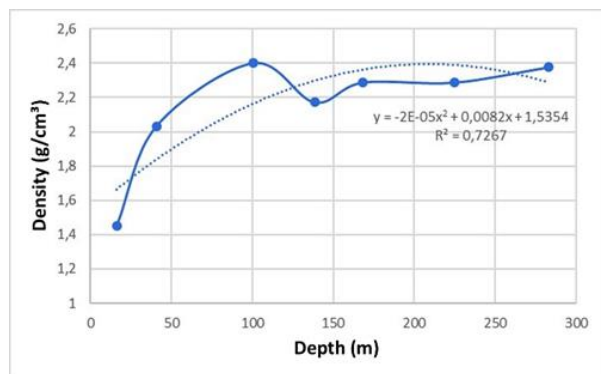


**Figure 11.** The calculated density values for SPAC 1 point.

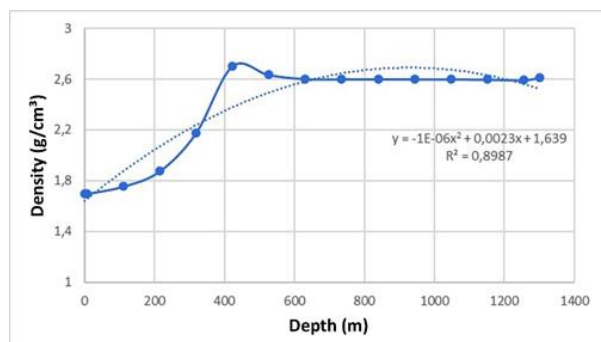


**Figure 12.** The density values along the A-A' profile for the SPAC 1 point.

From this perspective, density values were calculated based on the S-wave velocities obtained from SPAC measurements at two points up to an average depth of 300 meters. The density values were calculated using two empirical equations derived from the correlations between S-wave velocities and depth, as described in Figures 11 and 13. Additionally, cross-sections were taken from the 2D density model obtained through the inverse modeling techniques shown in Figure 9, and density values were similarly calculated as a function of depth, as depicted in Figures 12 and 14.

The main objective here is to make a comparative interpretation using microgravity density models that provide 2D and deeper information (depending on the length of the profile) in relation to the 1D and limited density models derived from SPAC measurements, and to examine the reliability of the results between the two methods as a function of depth, considering the correlation coefficients.

In the first step, the relationship between the calculated density values from SPAC 1 and SPAC 2 data for the depth range of 200-300 meters is presented in Figures 11 and 13. In the second step, the relationship between the density values obtained from microgravity measurements up to an average depth of 1400 meters at the points corresponding to the A-A' profile is calculated, as shown in Figures 12 and 14.

The calculations were performed using a second-degree polynomial function, which was found to be the most suitable trend function for the field data. The correlation coefficients were determined as 0.7267, 0.8987, 0.9574, and 0.8792, respectively.

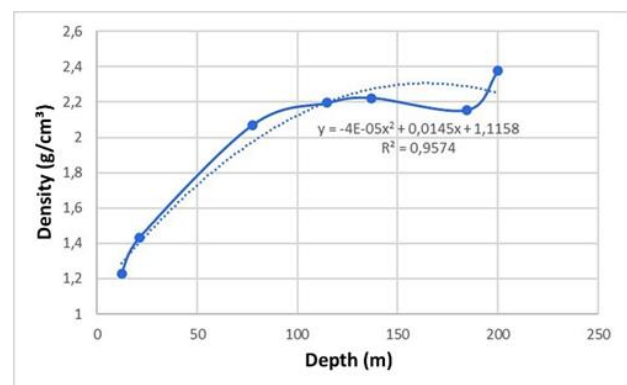


**Figure 13.** The calculated density values for SPAC 2 point.

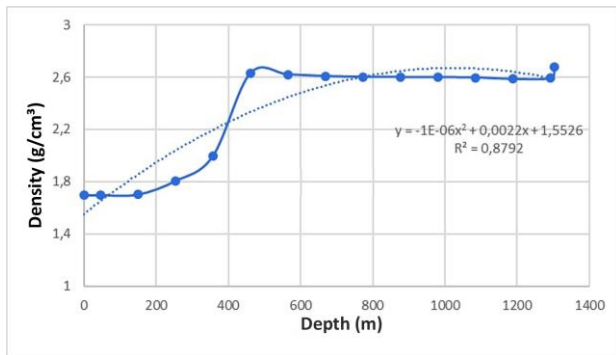


**Figure 14.** The density values along the A-A' profile for the SPAC 2 point.

#### 4. Discussions and Conclusions

In the study area located around the İzmir Bay, where in-situ geophysical methods were applied, the previous studies conducted using P and S wave velocities and density parameters (Akgün et al., 2013a; Akgün et al., 2013b; Özdağ et al., 2015; Pamuk et al., 2017; Pamuk et al., 2018; Özdağ et al., 2020; Özdağ and Gönenç, 2020) provide information about the subsurface layers. The expected thickness of the soil layers in the Bornova Plain is estimated to be around 300-350 m. In this study, the Modified Spatial Autocorrelation Method (MSPAC) applied by Özdağ in 2022 was used to obtain the S-wave velocities. Density values were calculated using the obtained S-wave velocities and depth information, and trend functions were calculated for each point by comparing them with the density model obtained from the inverse solution of the Bouguer gravity anomaly data. For the reliability test of the inverse solution algorithm, the anomaly created by a prism structure was calculated using flat solution methods and compared with the results obtained from the inverse solution algorithm. The comparison showed that the density and geometric parameters were successfully determined by the inverse solution algorithm. In the next step, regional residual separation was performed on the field data, and the residual Bouguer gravity anomaly was subjected to inverse solution. The density values calculated in the range of 1.65-2.85 g/cm<sup>3</sup> were found to be consistent with the previous studies conducted in the study area. Based on the inverse solution results, density distribution along the A-A' profile was calculated, and the density values obtained from the SPAC measurements given in Özdağ (2022) study were statistically analyzed. The calculated correlation coefficients indicate a compatibility of approximately 72% to 95% between the SPAC and microgravity density models in the study area. This approach demonstrates the usefulness of both methods in depth-controlled

analysis and provides insights into the estimation of deeper parameters. In light of these results, it is recommended to further investigate the mutual data validation through detailed statistical comparison studies in terms of data reliability. Also, The Bouguer correction process is more effective when obtaining Bouguer gravity anomalies, using the value of the crust density at the most suitable atmosphere-crust interface representing the region. Using the elevation values of the study area, reducing the topographic effects on Free Air Gravity anomaly data for various crustal density values can be achieved. Obtaining simple Bouguer Gravity anomalies for each applied density value and calculating their fractal dimensions will allow the calculation of higher resolution anomaly maps and, consequently, models (Erbek et al., 2020). When the results of the A-A' profile are examined, the observed concave base topography geometry is capable of focusing seismic waves on the surface. However, the SPAC study results do not present a homogeneous structure with depth for the S-wave velocities. Considering all these data and the damage caused by the 2020 Samos Earthquake (Çetin et al., 2022; Nuhuğlu et al., 2021), it is necessary to model the Bornova Plain in 3D at high resolutions and perform basin effect simulations based on this modeling.

#### Declaration of Ethical Standards

Authors declare that they adhere to all ethical standards.

#### Credit Authorship Contribution Statement

Author 1: Conceptualization, Methodology, Formal analysis, Investigation, Writing-original draft

Author 2: Conceptualization, Methodology, Formal analysis, Investigation, Writing-review and editing, Supervision, Project administration

#### Declaration of Competing Interest

The authors declare that they have no conflicts of interest concerning the content of this article.

#### Data Availability

All data created or analyzed during this study has been included in this published article.

#### Acknowledgment

The authors would like to thank Dokuz Eylül University Department of Scientific Research Projects 2021.KB.FEN.028 for some part of the microgravity data used in this study. Also, this study includes a part of Yaprak ÖZDAĞ's PhD Thesis at the Dokuz Eylül University The Graduate School of Natural and Applied Sciences Department of Geophysics Engineering.

## 5. References

- Akgün, M., Gönenç, T., Pamukçu, O., Özyalın, Ş., Özdağ, Ö.C. (2013a). Mühendislik Ana Kayasının Belirlenmesine Yönelik Jeofizik Yöntemlerin Bütünleşik Yorumu: İzmir Yeni Kent Merkezi Uygulamaları. *Jeofizik Dergisi*, **26**(2), 67-80.  
<https://doi.org/13.b02/jeofizik-1304-12>
- Akgün, M., Gönenç, T., Pamukçu, O. ve Özyalın, Ş. (2013b). Investigation of the relationship between ground and engineering bedrock at northern part of the Gulf of İzmir by borehole data supported geophysical Works. *Journal of Earth System Science*, **123**, 545-564  
<https://doi.org/10.1007/s12040-014-0414-3>
- Arisoy, M. Ö., Dikmen, Ü. (2011). Potensoft: MATLAB-based software for potential field data processing, modeling and mapping. *Computers & Geosciences*, **37**(7), 935-942.  
<https://doi.org/10.1016/j.cageo.2011.02.008>
- Asuero, A. G., Sayago, A., González, A. G. (2006). The correlation coefficient: An overview. *Critical reviews in analytical chemistry*, **36**(1), 41-59.  
<https://doi.org/10.1080/10408340500526766>
- Baker, K. (2005). Singular value decomposition tutorial. *The Ohio State University*, 4-24.
- Chen, W. Y., Li, H., Xue, G. Q., Chen, K., & Zhong, H. S. (2017). 1d Occam Inversion Of Sotem Data And its Application To 3d Models. *Chinese Journal Of Geophysics*, **60**(9), 3667-3676.  
<https://doi.org/10.6038/cjg20170930>
- Constable, S. C., Parker, R. L., & Constable, C. G. (1987). Occam's inversion: A practical algorithm for generating smooth models from electromagnetic sounding data. *Geophysics*, **52**(3), 289-300.  
<https://doi.org/10.1190/1.1442303>
- Çetin, K. O., Altun, S., Askan, A., Akgün, M., Sezer, A., Kincal, C., ... & Karaali, E. (2022). The site effects in İzmir Bay of October 30 2020, M7. 0 Samos earthquake. *Soil Dynamics and Earthquake Engineering*, **152**, 107051.  
<https://doi.org/10.1016/j.soildyn.2021.107051>
- Erbek, E., Öksüm, E., & Dolmaz, M.N. (2020). Orta Anadolu Bölgesi Atmosfer-Kabuk Ara Yüzeyi Kabuk Yoğunluğunun Fraktal Boyutlar İle Belirlenmesi. *Mühendislik Bilimleri ve Tasarım Dergisi*, **8**(3), 703-711.  
<https://doi.org/10.21923/jesd.717021>
- Erdoğan, B. (1990). İzmir-Ankara Zonu'nun İzmir ile Seferihisar arasındaki bölgede stratigrafik özellikleri ve tektonik evrimi. *TPJP Bülteni*, 1-20.
- Karadaş, A. (2014). Holocene Palaeogeographies and Coastline Changes of the Bornova Plain (İzmir). *Ege Coğrafya Dergisi*, **23**(2), 36-52.
- Kayan, İ. (2000). İzmir çevresinin morfotektonik birimleri ve alüvyonal Jeomorfolojisi, *Batı Anadolu Depremelliği Sempozyumu*, 103, 1-3
- Keçeli, A. (2009). Uygulamalı Jeofizik, TMMOB Jeofizik Mühendisleri Odası Eğitim Yayınları 9, 479.
- Li, X., & Chouteau, M. (1999). On density derived from borehole gravity. *The Log Analyst*, 40(01).  
<https://doi.org/SPWLA-1999-v40n1a3>
- Mukaka, M. M. (2012). A guide to appropriate use of correlation coefficient in medical research. *Malawi medical journal*, **24**(3), 69-71.
- Nuhoğlu, A., Erener, M. F., Hızal, Ç., Kincal, C., Erdoğan, D. Ş., Özdağ, Ö. C., Sezer, A. (2021). A reconnaissance study in İzmir (Bornova Plain) affected by October 30, 2020 Samos earthquake. *International Journal of Disaster Risk Reduction*, **63**, 102465.  
<https://doi.org/10.1016/j.ijdrr.2021.102465>
- Özdağ, Ö. C., Gönenç, T., Akgün, M. (2015). Dynamic amplification factor concept of soil layers: a case study in İzmir (Western Anatolia). *Arabian Journal of Geosciences*, **8**, 10093-10104.  
<https://doi.org/10.1007/s12517-015-1881-9>
- Özdağ, Ö. C., Gönenç, T. (2020). Modeling stratigraphic structure of Menemen Plain-Izmir/Turkey by microgravity, passive seismic methods and examining its behavior under earthquake effect. *Journal of Applied Geophysics*, **182**, 104175.  
<https://doi.org/10.1016/j.jappgeo.2020.104175>
- Özdağ, Ö., Akgün, M., Gönenç, T. (2020). Determining bedrock of the northern part of İzmir Bay, western Anatolia, using a combination of microtremor, ESPAC, VES, and microgravity methods. *Bollettino di Geofisica Teorica ed Applicata*, **61**(4).  
<https://doi.org/10.4430/bgta0313>
- Özdağ, Ö.C., (2022). Earthquake Based In-Situ Design Spectrum Creation by Using Geophysical Methods: İzmir Bay and Surrounding Area Example. PhD Thesis, Dokuz Eylül University, The School of Natural and Applied Sciences, Türkiye, 117 (In Turkish).

- Pamuk, E., Akgün, M., Özdağ, Ö. C., Gönenç, T. (2017). 2D soil and engineering-seismic bedrock modeling of eastern part of Izmir inner bay/Turkey. *Journal of Applied Geophysics*, **137**, 104-117.  
<https://doi.org/10.1016/j.jappgeo.2016.12.016>
- Pamuk, E., Gönenç, T., Özdağ, Ö. C., & Akgün, M. (2018). 3D bedrock structure of Bornova plain and its surroundings (Izmir/western Turkey). *Pure and Applied Geophysics*, **175**, 325-340.  
<https://doi.org/10.1007/s00024-017-1681-0>
- Pirttijavi M. (2008). User's Guide to Version Grablox 1,6b: Gravity Interpretation and Modelling Software based on a 3-D Block Model, *Department of Physics Universitas of Oulu Finland*. 3-57
- Ratner, B. (2009). The correlation coefficient: Its values range between+ 1/- 1, or do they?. *Journal of targeting, measurement and analysis for marketing*, **17**(2), 139-142.  
<https://doi.org/10.1057/jt.2009.5>
- Stewart, G. W. (1993). On the early history of the singular value decomposition. *SIAM review*, **35**(4), 551-566.  
<https://doi.org/10.1137/1035134>
- Taylor, R. (1990). Interpretation of the correlation coefficient: a basic review. *Journal of diagnostic medical sonography*, **6**(1), 35-39.  
<https://doi.org/10.1177/875647939000600106>
- Uzel, B., Sözbilir, H., Özkaymak, Ç. (2012). Neotectonic evolution of an actively growing superimposed basin in western Anatolia: The inner bay of Izmir, Turkey. *Turkish Journal of Earth Sciences*, **21**(4), 439-471.  
<https://doi.org/10.3906/yer-0910-11>
- Van Loan, C. F. (1976). Generalizing the singular value decomposition. *SIAM Journal on numerical Analysis*, **13**(1), 76-83.  
<https://doi.org/10.1137/0713009>